The Influence of Permanent Volumetric Deformation on the Reduction of the Load Bearing Capability of Plastic Components

P.A. Du Bois*, S. Kolling**, M. Feucht***, A. Haufe****
**Consultant, Freiligrathstr. 6, 63071 Offenburg, Germany*
***Gießen University of Applied Sciences, 35390 Gießen, Germany*
stefan.kolling@mmew.fh-giessen.de
****Daimler AG, EP/SPB, 71059 Sindelfingen, Germany*
markus.feucht@daimler.com
*****DYNAmore GmbH, Industriestrasse 2, 70565 Stuttgart, Germany*
andre.haufe@dynamore.de

Abstract

During the past years polymer materials have gained enormous importance in the automotive industry. Especially their application for interior parts to help in passenger safety load cases and their use for bumper fascias in pedestrian safety load cases have driven the demand for much more realistic finite element simulations. For such applications the material model 187 (i.e. MAT_SAMP-1) in LS-DYNA® has been developed.

In the present paper the authors show how the parameters for the rather general model may be adjusted to allow for the simulation of crazing effects during plastic loading. Crazing is usually understood as inelastic deformation that exhibits permanent volumetric deformations. Hence a material model that is intended to be applied for polymer components that show crazing effects during the experimental study, should be capable to produce the correct volumetric strains during the respective finite element simulation. The paper discusses the real world effect of crazing, the ideas to capture these effect in a numerical model and exemplifies the theoretical ideas with a real world structural component finite element model.

Introduction

Crazing is generally understood as the formation of micro cracks as sketched in Figure 1 (the micrograph is taken from [16]). As a consequence thereof, the change of color to white is visibly detectable since the crack-lengths become the magnitude of the wavelength of light. From a mechanical point of view, crazing leads to plastic (i.e. permanent) deformation accompanied by an increase of volume. Since surface cracks occur preferably under biaxial loading, crazing leads to low yield stress values in uniaxial/biaxial tension that can also be detected experimentally. It also seems to occur under high values of hydrostatic tension. In the present paper, the authors like to show how these effects can be captured in a phenomenological way by using non-isochoric plasticity and ductile damage.

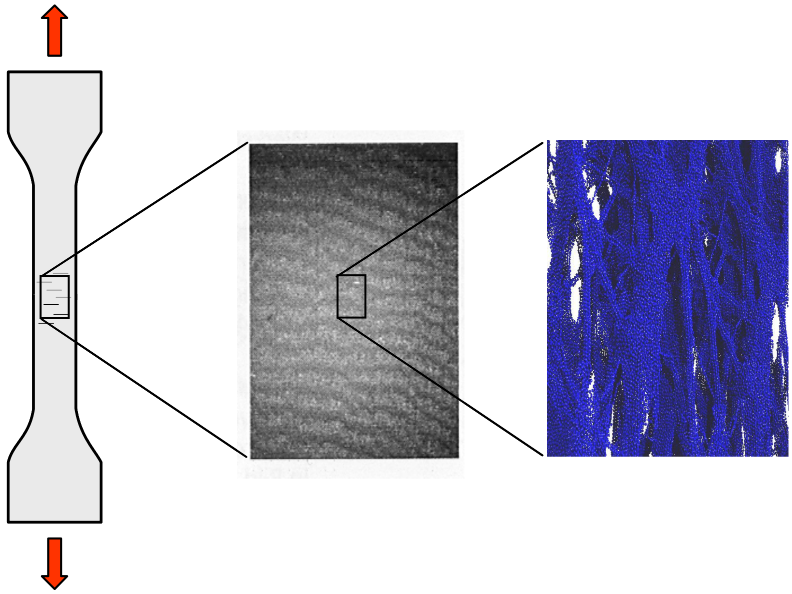

Figure 1: Formation of crazing

Numerical Treatment

In the present study, we used the SAMP-model suggested in [11]. This model combines non-isochoric plasticity and ductile damage. The advantage of this model is that all required input data may be provided in a tabulated way. Thus no parameter identification is necessary which represents an important factor in daily practice. See e.g. [13] for an overview of ductile damage models in LS-DYNA® in comparison with the tabulated damage model in SAMP. In what follows we give a short overview of the SAMP-model and the corresponding damage formulation.

Yield Surface and Plastic Potential in SAMP

The basic idea of SAMP is illustrated in Figure 2. Starting point is the definition of a pressure depending, quadratic yield surface

$$f\left(p,\sigma_{vm},\bar{\varepsilon}_p\right)=\sigma_{vm}^2-A_0-A_1p-A_2p^2\leq 0\ . \qquad (1)$$

This yield surface is defined by three independent stress states in the invariant plane following from tensile, compression, shear or biaxial stress for a fixed plastic strain during hardening. The hardening curve may be given in a tabulated way as it is well known from MAT_PIECE-WISE_LINEAR_PLASTICTY. The strain rate dependency is defined by tabulated tensile curves, i.e. the strain rate behaviour is assumed to be identically for all stress states. If less than three stress states are provided, the SAMP yield surface degenerates to a Drucker-Prager model (see [4], 2 curves are used) and a von Mises model (1 curve) respectively. Providing usually tensile, compression and shear data, the SAMP-coefficients are computed from the hardening curves internally by

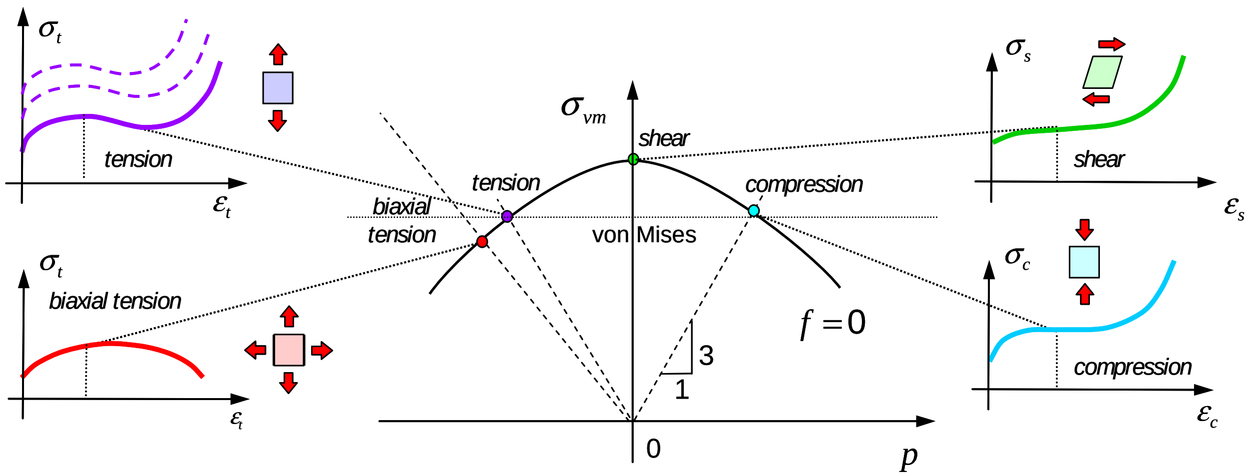

Figure 2: Yield surface in SAMP (Semi-Analytical Model for Polymers)

$$A_0 = 3\sigma_s^2 \quad A_1 = 9\sigma_s^2\left(\frac{\sigma_c - \sigma_t}{\sigma_c\sigma_t}\right) \quad A_2 = 9\left(\frac{\sigma_c\sigma_t - 3\sigma_s^2}{\sigma_c\sigma_t}\right)$$

In order to simulate crazing, the increase of volume during plastic flow is taken into account by defining the plastic potential

$$g = \sqrt{\sigma_{vm}^2 + \alpha p^2}\ . \tag{2}$$

The parameter α is determined internally if a plastic Poisson ratio ν_p (lateral strain rate over longitudinal strain rate) is provided by the user: i.e. either by a constant value or in a tabulated way as a function of longitudinal strain. In this context, it is also possible to define different behaviour under tension and compression. In the latter case, thermoplastics do not show volume increase so that it is recommended to define $\nu_p=0.5=const$ under pressure.

Damage Models in SAMP

The model uses the notion of the effective cross section, which is the true cross section of the material minus the cracks that have developed. We define the effective stress as the force divided by the effective cross section

$$\sigma = \frac{F}{A},\ \sigma_{eff} = \frac{F}{A_{eff}} = \frac{F}{A(1-d)} = \frac{\sigma}{1-d} \tag{3}$$

which allows defining an effective yield stress of $\sigma_{y,eff} = \dfrac{\sigma_y}{1-d}$. The damaged yield function in SAMP is given by

$$\Phi = \sigma_{vm}^2 - A_2 p^2 - (1-d)A_1 p - (1-d)^2 A_0 \tag{4}$$

By application of the principle of strain equivalence, stating that if the undamaged modulus is used, the effective stress corresponds to the same elastic strain as the true stress using the damaged modulus, one can write $E = \frac{\sigma_{eff}}{\varepsilon_e}, \quad E_d = \frac{\sigma}{\varepsilon_e} = E(1-d)$. Note that the plastic strains are therefore the same: $\varepsilon_p = \varepsilon - \frac{\sigma_{eff}}{E} = \varepsilon - \frac{\sigma}{E_d}$. No damage will occur under pure elastic deformation with this model. Among others, the damage model represents a good approximation to fit the unloading behavior of plastics [6]. A similar model is given by Lemaitre, where the damaged yield function is given by

$$\Phi = \sigma_{vm}^2 - (1-d)^2 \sigma_{y,eff}^2 (\varepsilon_{p,eff}) \ , \tag{5}$$

which leads to the same formulation as SAMP if we set $A_1 = A_2 = 0$ and $A_0 = \sigma_{y,eff}^2$. For a comparison of the chosen model with the formulation by Gurson we may rewrite

$$\Phi = \frac{\sigma_{vm}^2}{\sigma_{y,eff}^2} + 2q_1 f^* \cosh\left(\frac{q_2 - 3p}{2\sigma_{y,eff}}\right) - 1 - (q_1 f^*)^2 = 0 \ . \tag{6}$$

With $\cosh(x) \approx 1 + \frac{x^2}{2}$ we obtain a Taylor-approximation of Gurson's yield surface by

$$\Phi \approx \sigma_{vm}^2 + \frac{9}{4} q_1 f^* q_2^2 p^2 - (1 - q1 f^*)^2 \sigma_{y,eff}^2 \ . \tag{7}$$

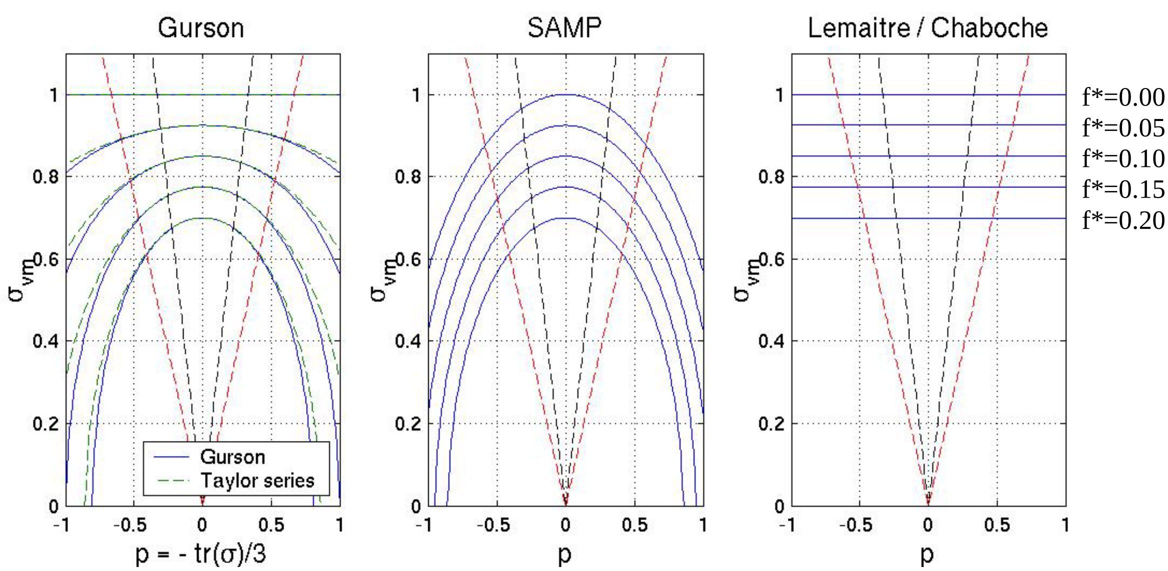

Figure 3: Evolution of the yield surface in function of damage in invariant plane

Comparison with Equation (4) yields the SAMP-parameters to be $d = q_1 f^*$, $A_0 = \sigma^2_{y,eff}$, $A_1 = 0$ and $A_2 = -\frac{9}{4} d q_2^2 \neq \text{const}$. Note that the last term is non-constant, i.e. the shape of the yield surface changes with increasing damage, see Figure 3. A comparison of the damage model in SAMP with Gurson's formulation, where Gurson's evolution law is approximated in SAMP by an equivalent tabulated input consisting of damage in function of plastic strain can be found in the study [15].

Application

As an industrial application we show a validation procedure for a structural part taken from a bumper that is made from PP T10. The experimental setup consists of a compression test on the structural component (Figure 4). In the picture in the middle, the formation of crazing can be observed very nicely. The intent of the present study is, on the one hand, to demonstrate the importance to consider the different behavior of thermoplastics under tension and compression. And, on the other hand, to represent crazing of the thermoplastic as it occurs in real-world-experiments.

Figure 4: Component test

In the first step, strain rate dependent tensile tests are performed and a material card is fitted solely from this tensile tests. We start our component validation with a standard material model in LS-DYNA: MAT_PIECEWISE_LINEAR_PLASTICTY (Mat No. 24). In order to investigate the mesh dependency we provide two meshes: A fine mesh (1mm element size) and a coarse mesh (6mm element size), see Figure 5.

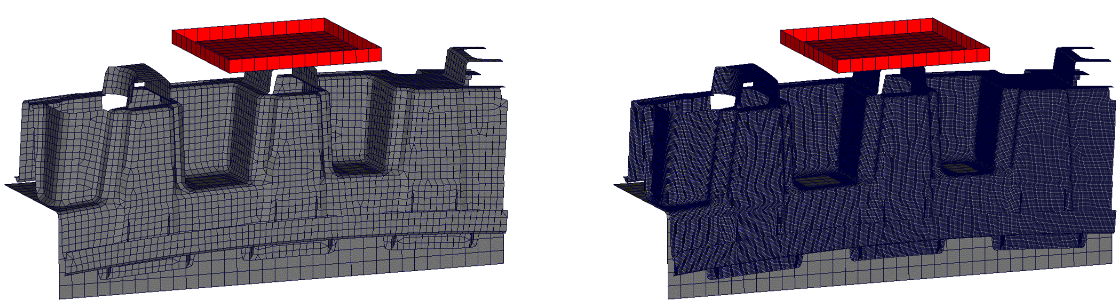

Figure 5: Coarse mesh (6mm element size) and fine mesh (1mm element size)

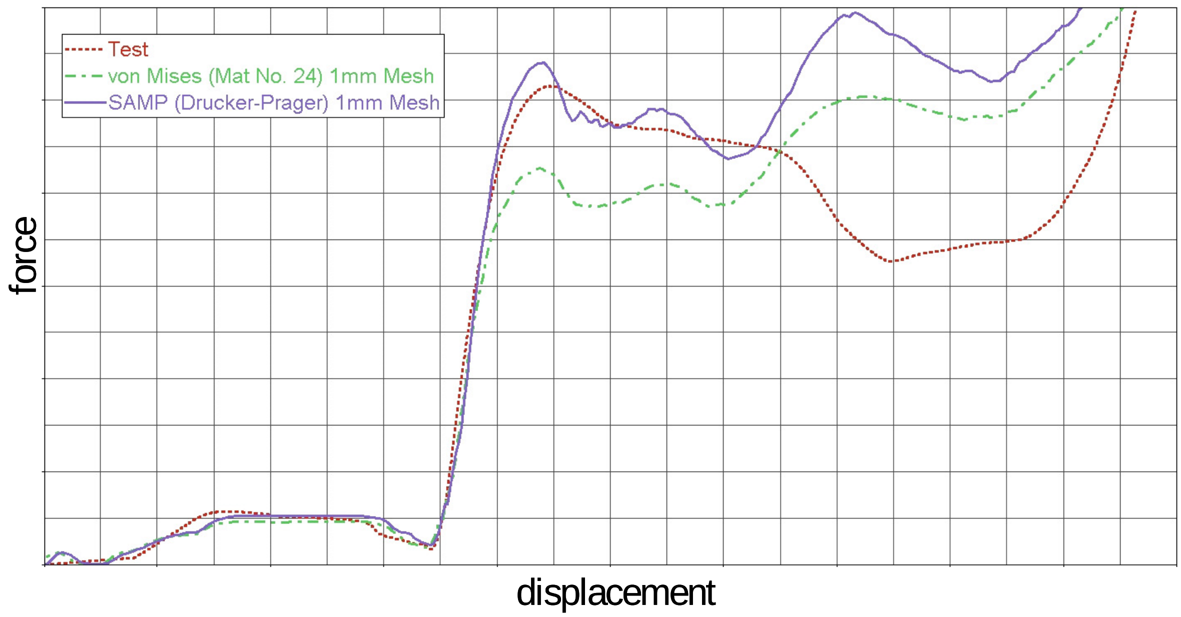

Figure 6: Force-displacement in comparison with the experiment: Mat No. 24 vs. SAMP

The problem of material cards which are fitted entirely under tension consists of the fact that there is no guarantee that it also works for multi-axial loading. In the present component test we have bending and, nearly exclusive, compression. The force-displacement-diagram in Figure 6 shows a typical behavior for thermoplastics: Material cards that are fitted for uniaxial tension yield a too soft response under bending and compression. Mat. No. 24 (dashed line) is therefore not capable to fit the experiment (dotted line) and, thus, different yield curves under compression and tension are necessary! This has been done in SAMP where a Drucker-Prager-model has been generated by scaling the tensile date by a factor 1.3 in the compressive region. This model is already in a very good agreement with the experimental data, though the range in the diagram where cracks occur are still too stiff. This is a topic of further investigation in near future.

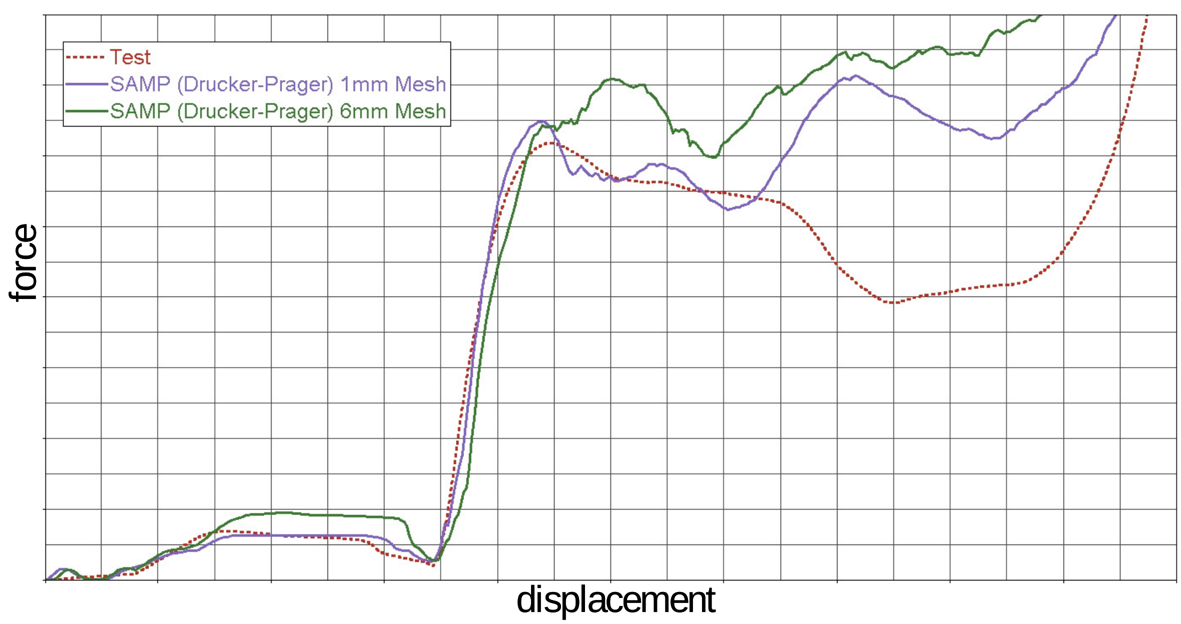

Figure 7: Influence of meshing

a) Mat. No. 24 b) SAMP

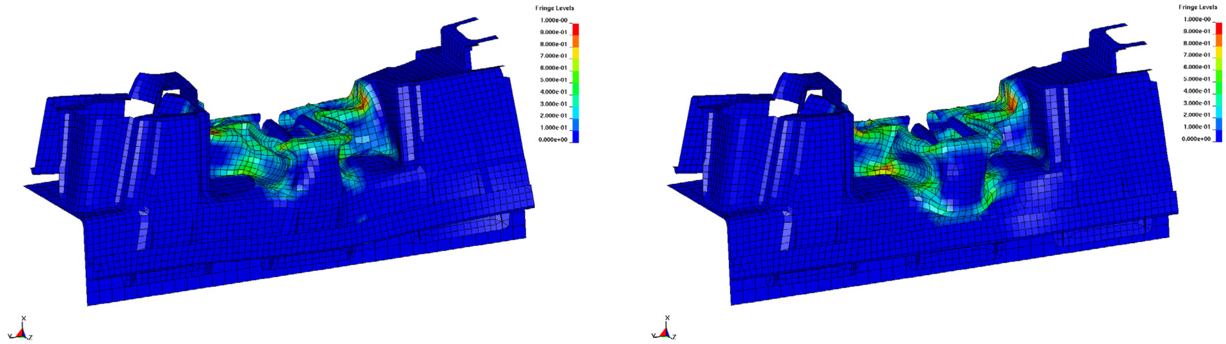

Figure 8: Crazing: Mat No. 24 vs. SAMP (coarse mesh)

Figure 7 shows the influence of using a coarse mesh and a fine mesh. As expected, the coarse mesh yields to a slightly stiffer response. This has also to be taking into account in full-car-simulations where the average element size is rather 5mm than 1mm. Further study has shown that mesh convergence will be reached for approximately 2mm element characteristic length.

At last, crazing of the component is approached by using the following SAMP-features:

– plastic Poisson's ratio decreases with increasing plastic strain (further input curve)
– plastic incompressibility under compression
– reduced biaxial strength (further input curve)
– damage evolution is considered (further input curve)

Figures 8 and 9 show the results of the simulation in comparison to Mat No. 24. As can be seen, the deformation behavior (see Figure 4) cannot be reproduced by using Mat No. 24. We obtain a totally different (and wrong) buckling mode. The simulation using SAMP together with the features described above yields to a quite more realistic deformation behavior. Moreover, the region of plastic volumetric strain (which is zero in Mat No. 24) represents a one-to-one relation to the region of crazing in the structural part. With other words, the effect of crazing cannot be simulated by any isochoric elasto-plastic material law! The craze deformation can be further improved by using the fine mesh (see Figure 9b).

a) Mat. No. 24 b) SAMP

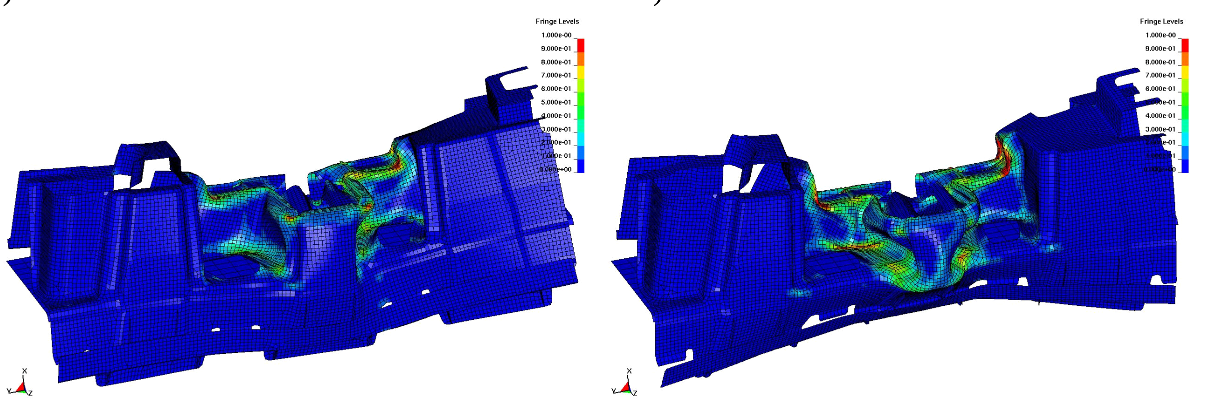

Figure 9: Crazing: Mat No. 24 vs. SAMP (fine mesh)

Summary and Outlook

Matching a measured force-displacement curve in a simulation should be phase 2 of the validation process. The numerical model will have a very limited range of validity unless the deformation (and failure) mode in the simulation correspond to what was observed. It seems useful to consider a coupling between damage and volumetric plastic strain in the simulation of thermoplastics. A combination of volumetric plastic strain, damage and reduced biaxial strength allowed to simulate the craze deformation in a rather complex structural part. The influence of crack formation and crack propagation is topic of further investigation in the near future.

References

[1] LS-DYNA®, Theory Manual / Keyword User's Manual, Livermore Software Technology Corporation.

[2] P.A. Du Bois: Crashworthiness Engineering Course Notes, Livermore Software Technology Corporation, 2004.

[3] S. Kolling, A. Haufe: A constitutive model for thermoplastic materials subjected to high strain rates, Proceedings in Applied Mathematics and Mechanics • PAMM 5: 303-304.

[4] D.C. Drucker, W. Prager: Soil mechanics and plastic analysis or limit design. Quaterly of Applied Mathematics, 10:157-165, 1952.

[5] V.A. Kolupaev, S. Kolling, A. Bolchoun, M. Moneke: A limit surface formulation for plastically compressible polymers. Mechanics of Composite Materials, 43(3):245--258, 2007.

[6] P. A. Du Bois, S. Kolling, M. Koesters, T. Frank: Material behavior of polymers under impact loading. International Journal of Impact Engineering 32 (2006) 725-740.

[7] J.C. Simo, T.J.-R. Hughes: Elastoplasticity and viscoplasticity – computational aspects. Springer Series in Applied Mathematics, Springer, Berlin, 1989.

[8] T.J.-R. Hughes: Efficient and simple algorithms for the integration of general classes of inelastic constitutive equations including damage and rate effects. In T.J.-R. Hughes, T. Belytschko: nonlinear finite element analysis course notes, 2003.

[9] J. Lemaitre, J.-L. Chaboche: Mécanique des matériaux solides, Dunod, 1988.

[10] W.W. Feng, W.H. Yang: general and specific quadratic yield functions, composites technology review.

[11] S. Kolling, A. Haufe, M. Feucht, P.A. Du Bois: A semianalytical model for the simulation of polymers. 4th LS-DYNA Forum, Germany 2005, Conference Proceedings, ISBN 3-9809901-1-7, pp. A-II-27/52.

[12] M. Vogler, R. Rolfes, S. Kolling: Orthotropic plasticity with application to fibre-reinforced thermoplastics. Proceedings of the 6th LS-DYNA Forum Meeting, Frankenthal, Germany, D-II:55-74, 2007.

[13] P.A. Du Bois, M. Feucht, S. Kolling, A. Haufe: An overview of ductile damage models in LS-DYNA. Proceedings of the 6th LS-DYNA Forum Meeting, Frankenthal, Germany, Keynote-Lectures I, pp 1-17, 2007.

[14] M. Vogler, S. Kolling and A. Haufe: A constitutive model for plastics with piecewise linear yield surface and damage. Proceedings of the 6th LS-DYNA Forum Meeting, Frankenthal, Germany, B-II:13-30, 2007.

[15] P.A. Du Bois, S. Kolling, M. Feucht, A. Haufe: A comparative review of damage and failure models and a tabulated generalization. Proceedings of the 6th European LS-DYNA Users Conference, Gothenburg, Sweden, pages 75-86, 2007.

[16] J. Rottler, M.O. Robbins: Growth, microstructure, and failure of crazes in glassy polymers, Phys Rev E, 68, 011801, 2003.